

High Frequency Gravitational Waves from Pulsar Timing Arrays

Junsong Cang^{1,*}, Yu Gao^{2,†}, Yiming Liu^{3,‡} and Sichun Sun^{3,§}

¹ School of Physics, Henan Normal University, Xinxiang, China

² Key Laboratory of Particle Astrophysics, Institute of High Energy Physics, Chinese Academy of Sciences, Beijing 100049, China and

³ School of Physics, Beijing Institute of Technology, Beijing, 100081, China

Several pulsar timing array (PTA) experiments such as NANOGrav and PPTA reported evidence of a gravitational wave background at the nano-Hz frequency band recently. This signal can originate from scalar-induced gravitational waves (SIGW) generated by the enhanced curvature perturbation. Here we perform a joint likelihood inference on PTA datasets, and our results show that if the PTA signals were indeed of SIGW origin, the curvature perturbations amplitude required will produce primordial black holes (PBHs) in $[2 \times 10^{-5}, 2 \times 10^{-2}] m_{\odot}$ mass range. Mergers of these PBHs can leave a strong gravitational wave signature in the $[10^{-3}, 10^8]$ Hz frequency range, to be detectable at upcoming interferometers such as the Einstein Telescope, DECIGO and BBO, etc. This offers a multi-frequency opportunity to further scrutinize the source of the observed PTA signal.

Introduction. Enthusiasm in primordial black holes (PBHs) [1, 2] has grown immensely after the LIGO discovery of gravitational wave signals [3] in agreement with merger events of black holes above stellar masses [4]. With sufficiently large primordial curvature perturbation \mathcal{R} , such black holes can be produced in the early Universe from gravitational collapse of overdense regions. PBHs are under extensive searches for their astrophysical signals, see Ref. [5] for a recent review. The early process of over-density collapse is also predicted to emit scalar-induced gravitational waves (SIGW) [6, 7], which offers a glimpse at valuable information of early fluctuations at late-time gravitational wave detectors.

In recent months, several Pulsar Timing Arrays (PTAs) observatories including NANOGrav [8], Chinese PTA (CPTA) [9], Parkes PTA (PPTA) [10] and European PTA [11, 12] reported strong evidence for gravitational wave (GW) background at the nano-Hertz waveband, which verifies previous claims [13–16]. These observations incited extensive studies on potential sources of the observed GW background [17–23], including supermassive black holes [24–26], merging PBHs [27, 28], phase transitions [29–32] and axion topological defects [33–35], etc.

As a viable nano-Hz source, an SIGW-emitting overdensity collapse process generally requires a curvature power spectrum $P_{\mathcal{R}}$ with a large amplitude at the scale of $k \sim 10^8 \text{ Mpc}^{-1}$ [17, 24] to be consistent with the PTA data. Although $P_{\mathcal{R}}$ is strictly constrained at large scales ($k \lesssim 10 \text{ Mpc}^{-1}$) by observations of cosmic microwave background (CMB) and large scale structures [36, 37], $P_{\mathcal{R}}$ can still assume a large value at smaller scales [7] and it can potentially assume an amplitude to explain the PTA signal.

In this letter, we show that high-frequency GWs are predicted from an SIGW generating $P_{\mathcal{R}}$ amplitude in consistency with the PTA data. A perturbation spectrum that yields the required nano-Hertz gravitational wave will also lead to the formation of PBHs with mass in $[2 \times 10^{-5}, 2 \times 10^{-2}] m_{\odot}$ range, and the mergers of these PBHs produce a GW background peaked at around MHz frequencies. Such a high-frequency GW signal shall be readily detectable at various upcoming observatories such as Einstein Telescope (ET) [38], Deci-Hertz Interferometer Gravitational Wave Observatory (DECIGO) [39] and Big Bang Observer (BBO) [40]. Since the endeavor of the whole gravitational wave frequency spectrum searches has begun, with various proposals already in MHz-GHz band [41–44], cross-linking the ultralow nano-Hz gravitational waves to the ultrahigh-frequency searches in a multi-messenger task in the GW spectrum space is intriguing.

We will first briefly review our model for SIGW and merging PBH, the inference settings, and then we perform a scan over the relevant PBH parameter space to obtain the upper boundary of the predicted high-frequency GW. We will show that the currently allowed GW signal range in consistency with existing PBH limits can be well probed by future interferometry experiments.

GW signal. We consider a log-normal curvature power spectrum [17, 24, 45–47] as a good representative for a large class of curvature perturbation models that feature a characteristic perturbation scale,

$$P_{\mathcal{R}} = \frac{A}{\sqrt{2\pi}\Delta^2} \exp\left[-\frac{(\ln k/k_*)^2}{2\Delta^2}\right], \quad (1)$$

where A , k_* and Δ are model parameters, which describe the amplitude, peak location and the width of $P_{\mathcal{R}}$ respectively. Upon horizon crossing, $P_{\mathcal{R}}$ will modify the radiation quadrupole moment and generate SIGW at second order. A sufficiently large $P_{\mathcal{R}}$ will also create overdense regions that collapse gravitationally and form PBHs [7]. Here we find that the PBH mass distribution generated from the spectrum in Eq. (1) can be well parameterized

*Electronic address: cangjunsong@outlook.com

†Electronic address: gaoyu@ihep.ac.cn

‡Electronic address: 7520220161@bit.edu.cn

§Electronic address: sichunssun@bit.edu.cn

by a log-normal profile [7],

$$\psi \equiv \frac{df_{\text{bh}}}{d \ln m} = \frac{f_{\text{bh}}}{\sqrt{2\pi}\sigma_{\text{bh}}} \exp \left[-\frac{\ln^2(m/m_c)}{2\sigma_{\text{bh}}^2} \right], \quad (2)$$

where $f_{\text{bh}} \equiv \rho_{\text{bh}}/\rho_{\text{dm}}$ is the fraction of DM made of PBHs, ρ_{bh} and ρ_{dm} denote mass densities of PBH and DM respectively. m denotes PBH mass, m_c and σ_{bh} are peak and width of the distribution respectively. After their production, PBHs can form binary systems which subsequently merge and emit GW at higher frequencies. The comoving merger rate R of a pair of PBHs with mass m_1 and m_2 is given by [48],

$$\begin{aligned} \frac{dR}{dm_1 dm_2} &\simeq \frac{1.6 \times 10^6}{\text{Gpc}^3 \text{ yr}} f_{\text{bh}}^{-\frac{21}{37}} \eta^{-\frac{34}{37}} \left(\frac{M}{m_\odot} \right)^{-\frac{32}{37}} \\ &\times \left(\frac{t}{t_0} \right)^{-\frac{34}{37}} S \psi(m_1) \psi(m_2) \end{aligned} \quad (3)$$

where $M = m_1 + m_2$, $\eta = m_1 m_2 / M^2$ and t is the time of the merger. $t_0 = 13.8$ Gyr is the current age of the Universe. S is a suppression factor and we take its form from Ref [48, 49]:

$$S = \frac{e^{-\bar{N}(y)}}{\Gamma(21/37)} \int dv v^{-\frac{16}{37}} \exp \left[-\phi - \frac{3\sigma_M^2 v^2}{10f_{\text{bh}}^2} \right], \quad (4)$$

$$\phi = \frac{\bar{N}(y) \langle m \rangle}{f_{\text{bh}}} \int \frac{dm}{m} \psi(m) F \left(\frac{M}{\langle m \rangle} \frac{v}{\bar{N}(y)} \right), \quad (5)$$

where $\sigma_M \simeq 0.004$, $\bar{N}(y)$ is the expected number of PBHs within a comoving radius of y around the binary [50], and we take $\bar{N}(y) \simeq M f_{\text{bh}} / [\langle m \rangle (f_{\text{bh}} + \sigma_M)]$ following [48–50]. This choice has been shown to be in agreement with numerical simulations for $f_{\text{bh}} \leq 0.1$ [48, 50]. $\langle m \rangle$ is the mean of PBH mass over number density distribution [49], which equals $m_c e^{-\sigma_{\text{bh}}^2/2}$ for our log-normal mass distribution in Eq. (2). $F(z) = {}_1F_2(-1/2, 3/4, 5/4; -9z^2/16) - 1$, and ${}_1F_2$ is the generalized hypergeometric function.

The energy density for merging PBHs is calculated as [27],

$$\Omega_{\text{GW}} = \frac{f}{\rho_{\text{cr}}} \int \frac{dz}{(1+z)} \frac{dR}{H} \frac{dE_{\text{GW}}(f_r)}{df_r} \quad (6)$$

here $\Omega_{\text{GW}} \equiv \rho_{\text{cr}}^{-1} d\rho_{\text{GW}}/d \ln f$ is fractional GW density per log frequency interval, ρ_{GW} and ρ_{cr} are GW density and current critical density respectively, $f_r = (1+z)f$ is the source frequency, $dE_{\text{GW}}(f_r)/df_r$ is the source energy spectrum for each PBH merger event, for which we adopt [51], $H = H_0[\Omega_\Lambda + \Omega_m(1+z)^3 + \Omega_r(1+z)^4]^{1/2}$ is Hubble parameter in the Λ CDM cosmology. For parameter values we adopt the Planck 2018 results [37] of $H_0 = 67.66 \text{ kms}^{-1} \text{ Mpc}^{-1}$, $\Omega_\Lambda = 0.6903$, $\Omega_m = 0.3096$, and we assume massless neutrinos such that the radiation density fraction is $\Omega_r = 9.1 \times 10^{-5}$.

Inference Settings. Here we analyze the PTA datasets using our SIGW signal to map out the credible region of PBH parameters and that for the associated high-frequency merger signal. Our log-likelihood is

$$\ln \mathcal{L} = -\frac{1}{2} \sum_i \frac{(x_i - u_i)^2}{\sigma_i^2}, \quad (7)$$

here the index i denotes frequency, x is Ω_{GW} for our SIGW model, u is the measured median for Ω_{GW} , and $\sigma \in \{\sigma_u, \sigma_l\}$ which represents the upper or lower error bars for Ω_{GW} , respectively. We use datasets from NANOGrav-15 [8], IPTA [16] and PPTA [10] in our inference, and we follow Ref. [17] and estimate the signal median and error bars for each experiment directly using the Ω_{GW} posterior summarised in Ref. [18, 22]. For validation, we have checked that our fitting agrees very well with Ref. [17] and [24] when using NANOGrav-15 data alone.

As a contributor to dark radiation, the extra energy budget in SIGW will also change the effective degree of relativistic degrees of freedom N_{eff} . In Planck 2018 results (hereafter PLK) [37], a joint analysis of datasets from CMB, baryon acoustic oscillations (BAO) and Big Bang Nucleosynthesis (BBN) presented an upper limit [7, 37]

$$\Delta N_{\text{eff}} \equiv N_{\text{eff}} - 3.046 \leq 0.175, \text{ 95\% C.L.}, \quad (8)$$

here 3.046 is the value of N_{eff} predicted by the standard model of particle physics [7, 37, 52]. This N_{eff} constraint translates into an upper bound on the integrated GW density, or $\int d \ln f \Omega_{\text{GW}} < 2.1 \times 10^{-6}$ [7].

To accommodate the PLK N_{eff} limits, we add a $\Delta N_{\text{eff}} < 0.175$ prior to our inference. Since f_{bh} in our mass range has been constrained to $\mathcal{O}(0.1)$ [53], we also use a prior of $f_{\text{bh}} \in [10^{-20}, 0.1]$ to ensure that PBH does not violate the existing abundance constraints while maintaining a physically meaningful abundance for appreciable merger GW production. Given all the discussions above, we consider three benchmark inference settings:

- **GW:** Use PTA GW data alone.
- **GW + ΔN_{eff} :** Use PTA GW data and PLK ΔN_{eff} limits in Eq. (8).
- **GW + ΔN_{eff} + PBH:** Use PTA GW data and PLK ΔN_{eff} limits along with the prior of $f_{\text{bh}} \in [10^{-20}, 10^{-1}]$.

Results. We sample the $P_{\mathcal{R}}$ parameter space with the likelihood in Eq. (7) using the `multinest` sampler [54], and we compute constraints for our $P_{\mathcal{R}}$ parameters and various derived observables (e.g. ΔN_{eff} , PBH parameters and merger GW) by analyzing the `multinest` chains using the `GetDist` package [55]. Table I summarises the prior ranges for our parameters along with their marginalized confidence region. Fig. 1 visualizes the

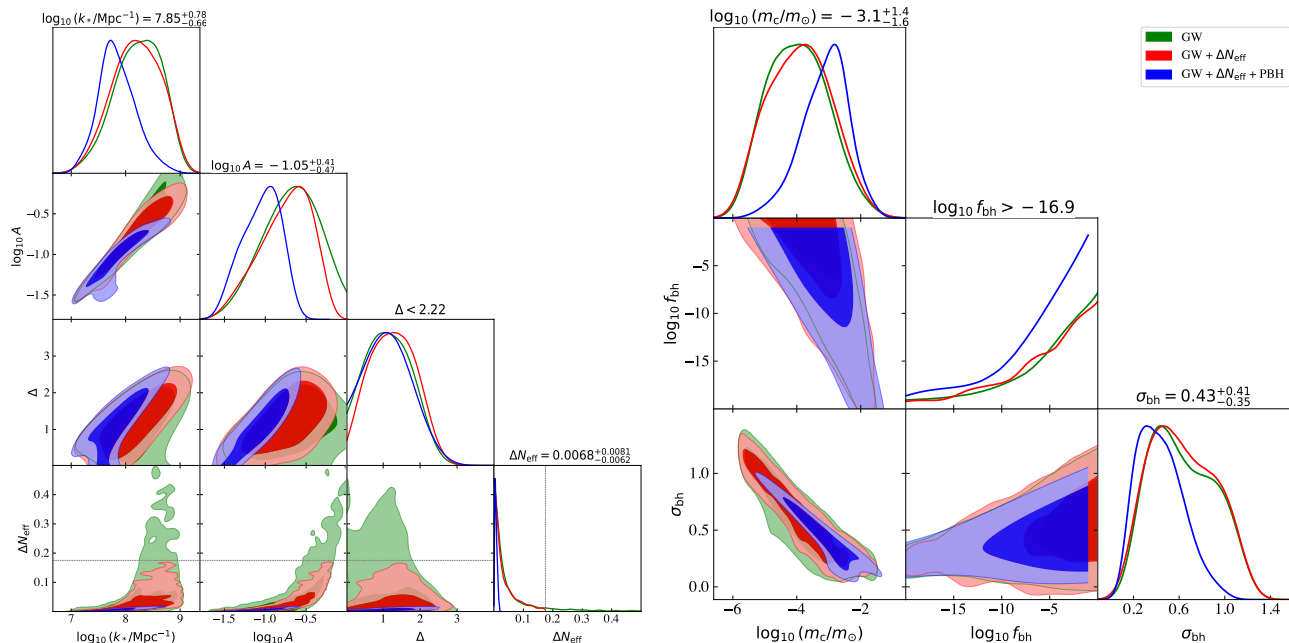


FIG. 1: Marginalised posteriors for our $P_{\mathcal{R}}$ parameters (k_* , A , Δ) and the derived ΔN_{eff} and PBH parameters (m_c , f_{bh} , σ_{bh}). The green, red, and blue contours correspond to GW, GW + ΔN_{eff} , and GW + ΔN_{eff} + PBH inference settings respectively. Light and dark-shaded regions correspond to 68% and 95% confidence levels respectively. The dotted line in the ΔN_{eff} panels indicates the PLK upper limit of $\Delta N_{\text{eff}} < 0.175$, and numbers on the diagonal panels show the marginalized mean and 95% confidence region from our main GW + ΔN_{eff} + PBH setting.

Parameters	Prior range	95% Limits	
		GW	GW+ ΔN_{eff} + PBH
$\log_{10} A$	$[-1.8, 0]$	$[-1.3, -0.0]$	$[-1.51, -0.63]$
$\log_{10}(k_*/\text{Mpc}^{-1})$	$[6.8, 9.0]$	$[7.4, 9.0]$	$[7.2, 8.6]$
Δ	$[0.02, 4]$	$[0.02, 2.2]$	$[0.02, 2.22]$
$\log_{10} f_{\text{bh}}$	$[-20, -1]$	$[-13.6, 10.2]$	$[-16.9, -1]$
$\log_{10}[m_c/m_{\odot}]$	–	$[-5.7, -2.1]$	$[-4.7, -1.7]$
σ_{bh}	–	$[0.15, 1.17]$	$[0.08, 0.84]$
ΔN_{eff}	≤ 0.175	$[0, 0.36]$	$[0.006, 0.014]$

TABLE I: Parameters in our inference and their allowed range and marginalized 95% C.L. limits. A , k_* and Δ are our free model parameters, whereas f_{bh} , m_c , σ_{bh} and ΔN_{eff} are parameters derived from A , k_* and Δ . Note that fitting to GW data alone may overproduce PBHs without an f_{bh} prior.

marginalized posterior from our inference, in which the left panel shows the results for our $P_{\mathcal{R}}$ model parameters and the derived ΔN_{eff} from different inference settings, and the right panel shows the results for PBH parameters f_{bh} , m_c and σ_{bh} .

As illustrated in the left panel of Fig. 1 and from Table I, using GW data alone gives a marginalized ΔN_{eff} 95% C.L. upper bound of 0.36, which is about 2σ away from the PLK upper limit, and adding the prior in Eq. (8) leads to a tighter constraint. With both inference settings, the derived posterior for f_{bh} can reach beyond the

physically forbidden region of $f_{\text{bh}} \geq 1$ and the physically motivated $f_{\text{bh}} < 0.1$ prior tightens the parameter space significantly. In the fitting with GW data, m_c and σ_{bh} are constrained (at 95% C.L.) to $[1.8 \times 10^{-6}, 7.5 \times 10^{-2}] m_{\odot}$ and $[0.15, 1.17]$ respectively. In GW+ ΔN_{eff} +PBH fitting, the constraint tightens to $[2 \times 10^{-5}, 2 \times 10^{-2}] m_{\odot}$ for m_c and $[0.08, 0.84]$ for σ_{bh} .

In the green-colored regions of Fig. 2, we show the 95% C.L. posterior for the merger GW (left) and merger rate (right) derived from our main GW+ ΔN_{eff} +PBH inference, and the black solid curves correspond to the maximum likelihood best-fit values of $f_{\text{bh}} = 0.1$, $m_c = 2.6 \times 10^{-4} m_{\odot}$ and $\sigma_{\text{bh}} = 0.54$. Our Ω_{GW} posterior peaks at around 10 MHz with an amplitude of $\mathcal{O}(10^{-8})$, which potentially falls into the frequency range of various high-frequency proposals [41–43]. Towards lower frequencies Ω_{GW} decays as $f^{2/3}$, and below 10^4 Hz, Ω_{GW} starts to fall into the sensitivity reach of various proposed experiments [6, 63, 64], such as Cosmic Explorer (CE) [59], Einstein Telescope (ET) [38], Deci-Hertz Interferometer Gravitational Wave Observatory (DECIGO) [39] and Big Bang Observer (BBO) [40]. For DECIGO and BBO in particular, Ω_{GW} posterior strength exceeds the sensitivity reach by about a factor of 10^3 and 10^5 , indicating a positive prospect for experimental searches. The right panel of Fig. 2 shows that our inference constrains the merger rate today to $R \lesssim 4 \times 10^7 \text{ Gpc}^3 \text{ yr}^{-1}$. Since $R \propto t^{-34/37}$ (see Eq. (3)) and that $t \propto (1+z)^{-1.49}$ for $z \in [0, 200]$, our posterior for R scales roughly as

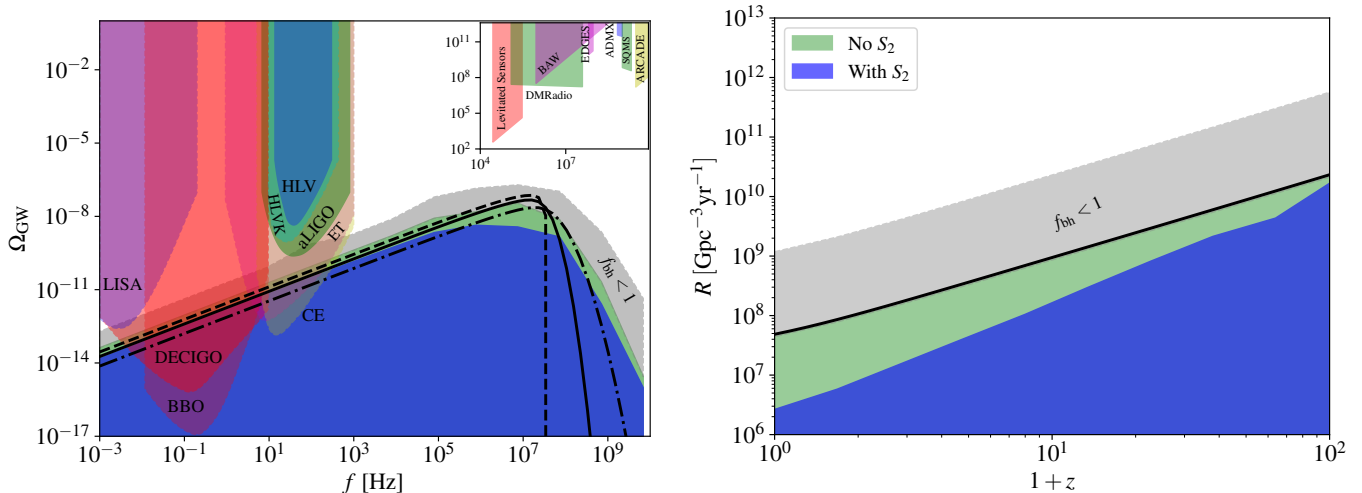


FIG. 2: 95% C.L. confidence region for merger Ω_{GW} (left) and merger rate (right) from GW + ΔN_{eff} + PBH inference, legend applies to both panels. The green (blue) regions show the posterior when halo disruption of PBH binary (see Eq. (9)) is ignored (considered). We also show results when $f_{\text{bh}} < 0.1$ prior is lifted to $f_{\text{bh}} < 1$ (ignoring the S_2 term in Eq. (9)), however for $f_{\text{bh}} > 0.1$ the robustness of our merger calculation is yet to be verified, thus we mark these regimes with grey regions. The solid black lines correspond to our best-fit PBH parameters of $f_{\text{bh}} = 10^{-1}$, $m_c = 2.6 \times 10^{-4} m_{\odot}$, $\sigma_{\text{bh}} = 0.54$. In the left panel, we also show Ω_{GW} computed for $\sigma_{\text{bh}} = 0$ (monochromatic PBHs, dashed) and $\sigma_{\text{bh}} = 1$ (dot-dashed), with the f_{bh} and m_c fixed to 0.1 and $2.6 \times 10^{-4} m_{\odot}$ respectively. We also illustrate the landscape of experimental sensitivities from various GW observatories operating in our frequency window. The experimental reach for LISA [56], DECIGO [57], BBO [58], ET [38], CE [59], aLIGO [60], HLVK [24] (a detector network consisting of aLIGO in Hanford and Livingston [60], aVIRGO [61] and KAGRA [62]) and HLV [24] (similar to HLVK but without KAGRA) are the power law integrated sensitivities [63] from Refs [6, 24, 63, 64]. The sensitivities for Levitated Sensors [65], bulk acoustic wave (BAW) [66], DMRadio [67], EDGES [68], ADMX [69], SQMS [70] and ARCADE [71] (shown in the inset) are adapted from [72]. We adopt design sensitivity for HLVK and third observation run for HLV [24]. Existing and projected experimental limits are indicated by solid and dashed edges, respectively.

$$R \propto (1+z)^{1.4}.$$

In both panels, we also show the results with a relaxed prior $f_{\text{bh}} < 1$ (grey), equivalent to a requirement that PBH does not exceed the total dark matter density, with the caveat that the $\bar{N}(y)$ formulation needs validation in the $f_{\text{bh}} > 0.1$ region [48, 50]. Fig. 2 shows that in this relaxed case, the Ω_{GW} posterior increases by about a factor of 5, and the GW signals fall into the sensitivity reach of advanced LIGO (aLIGO) [64] and LISA (Laser Interferometer Space Antenna) [73], whereas the posterior for merger rate R is raised by about a factor of 26.

After structure formation begins, PBH binaries may collide with DM halos containing PBH clusters [49, 74], which disrupts the binary and thereby suppresses the PBH merger rate at lower redshifts. This effect can be accounted for by multiplying the differential merger rate in Eq. (3) by an additional suppression term S_2 [49],

$$S_2 \simeq \min [1, 1.96 \times 10^{-3} x^{-0.65} \exp(0.03 \ln^2 x)] \quad (9)$$

here $x = (t/t_0)^{0.44} f_{\text{bh}}$. We show results for this scenario in the blue contours of Fig. 2, and it can be seen that this lowers Ω_{GW} posterior by about a factor of 3, and the corresponding posterior for merger rate today is reduced to about $R \lesssim 2.6 \times 10^6 \text{ Gpc}^3 \text{ yr}^{-1}$.

Summary. Enhanced curvature perturbation $P_{\mathcal{R}}$ can

produce SIGW which serves as a good source candidate of the GW signal recently reported by various PTA experiments. This letter scrutinizes the implication of this scenario at the higher frequency band of the GW spectrum. We performed extensive inference analysis of PTA GW datasets in combination with existing constraints on integrated GW density (parameterized by ΔN_{eff}) and PBH abundance, from which we map out posterior distributions for PBHs and relevant merger GW signals, and we show that if the PTA GW signal were indeed sourced by SIGW, the $P_{\mathcal{R}}$ amplitude required will create PBHs in $[2 \times 10^{-5}, 2 \times 10^{-2}] m_{\odot}$ mass range. Mergers of these PBHs will produce strong GW background across $[10^{-3}, 10^8]$ Hz frequencies, which falls into the sensitivity reach of various proposed GW projects such as the Einstein Telescope (ET), Cosmic Explorer (CE), DECIGO and BBO, thus GW experiments can help verify the SIGW scenario for PTA gravitational waves.

Acknowledgements. The authors thank Gabriele Franciolini and Paul Frederik Depta for their helpful discussions. This work is supported by the National Natural Science Foundation of China (No. 12105013 and No. 12275278).

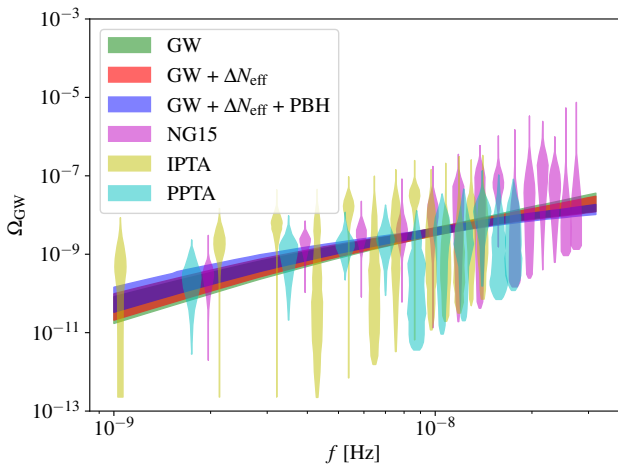


FIG. 3: Posterior distribution of SIGW and a comparison with experimental data. The green, red, and blue regions show our 68% C.L. posterior for SIGW from different inference settings, and the magenta, yellow and cyan regions show the measured Ω_{GW} posterior for NANOGrav 15 years result (NG15) [8], IPTA [16] and PPTA [10].

Appendix A: Production of SIGW and PBHs from curvature perturbation

Upon horizon crossing, $P_{\mathcal{R}}$ will modify the radiation quadrupole moment and generate SIGW at second order, whose energy density per log frequency interval today is given by [7, 45, 75, 76]

$$\begin{aligned} \Omega_{\text{GW}} &\equiv \frac{1}{\rho_{\text{cr}}} \frac{d\rho_{\text{GW}}}{d \ln f} \\ &= 0.29 \Omega_{\text{r}} \left(\frac{106.75}{g_*} \right)^{1/3} \\ &\quad \times \int_0^\infty dv \int_{|1-v|}^{1+v} du \left[\frac{4v^2 - (1 - u^2 + v^2)^2}{4u^2 v^2} \right]^2 \\ &\quad \times \left(\frac{u^2 + v^2 - 3}{2uv} \right)^4 F(u, v) P_{\mathcal{R}}(kv) P_{\mathcal{R}}(ku), \end{aligned} \quad (\text{A1})$$

$$\begin{aligned} F(u, v) &= \left(\ln \left| \frac{3 - (u + v)^2}{3 - (u - v)^2} \right| - \frac{4uv}{u^2 + v^2 - 3} \right)^2 \\ &\quad + \pi^2 \Theta(u + v - \sqrt{3}), \end{aligned} \quad (\text{A2})$$

g_* is the total degree of freedom for massless particles when the mode k enters horizon ($k = aH$) [77, 78], Θ is the Heaviside step function, and the frequency f is related to the wavenumber k via [47],

$$f = 1.546 \times 10^{-15} \left(\frac{k}{\text{Mpc}^{-1}} \right) \text{Hz} \quad (\text{A3})$$

In Fig. 3 we illustrate the comparison of PTA data and SIGW posteriors from our inferences.

In addition to emitting SIGW, sufficiently large $P_{\mathcal{R}}$ will also generate overdense regions that can gravitationally collapse into PBHs with mass [7, 47, 79–81],

$$m = 2.43 \times 10^{-4} \left(\frac{\gamma}{0.2} \right) \left(\frac{g_*}{106.75} \right)^{-1/6} \left(\frac{k}{10^8 \text{Mpc}^{-1}} \right)^{-2} m_{\odot}, \quad (\text{A4})$$

here γ is the collapse efficiency, for which we adopt a typical value of $\gamma = 0.2$ following [47, 79, 81]. The corresponding distribution of PBH abundance is given by [53, 81–83],

$$\begin{aligned} \psi &\equiv \frac{df_{\text{bh}}}{d \ln m} \\ &= 0.28 \left(\frac{\beta}{10^{-8}} \right) \left(\frac{\gamma}{0.2} \right)^{3/2} \left(\frac{g_*}{106.75} \right)^{-1/4} \left(\frac{m}{m_{\odot}} \right)^{-1/2}, \end{aligned} \quad (\text{A5})$$

where

$$\beta(m) \simeq \sqrt{\frac{2\bar{\sigma}^2}{\pi\delta_c^2}} \exp\left(-\frac{\delta_c^2}{2\bar{\sigma}^2}\right), \quad (\text{A6})$$

$$\bar{\sigma}^2(m) = \frac{16}{81} \int d \ln k' \left(\frac{k'}{k} \right)^4 P_{\mathcal{R}}(k') W^2 \left(\frac{k'}{k} \right), \quad (\text{A7})$$

here δ_c is the threshold for gravitational collapse, for which we adopt 0.45 following [7, 53, 84, 85]. $W(x)$ is a window function, which we use $\exp(-x^2/2)$ [7, 47, 81].

-
- [1] Y. B. Zel'dovich and I. D. Novikov, Soviet Astron. AJ (Engl. Transl.), **10**, 602 (1967).
[2] B. J. Carr and S. W. Hawking, Mon. Not. Roy. Astron. Soc. **168**, 399 (1974).
[3] B. P. Abbott et al. (LIGO Scientific, Virgo), Phys. Rev. X **9**, 031040 (2019), 1811.12907.
[4] S. Bird, I. Cholis, J. B. Muñoz, Y. Ali-Haïmoud,

- M. Kamionkowski, E. D. Kovetz, A. Raccanelli, and A. G. Riess, Phys. Rev. Lett. **116**, 201301 (2016), 1603.00464.
[5] B. Carr and F. Kuhnel, SciPost Phys. Lect. Notes **48**, 1 (2022), 2110.02821.
[6] G. Domènech, Universe **7**, 398 (2021), 2109.01398.
[7] J. Cang, Y.-Z. Ma, and Y. Gao, Astrophys. J. **949**, 64

- (2023), 2210.03476.
- [8] G. Agazie et al. (NANOGrav), *Astrophys. J. Lett.* **951**, L8 (2023), 2306.16213.
- [9] H. Xu et al., *Res. Astron. Astrophys.* **23**, 075024 (2023), 2306.16216.
- [10] D. J. Reardon et al., *Astrophys. J. Lett.* **951**, L6 (2023), 2306.16215.
- [11] J. Antoniadis et al. (EPTA) (2023), 2306.16226.
- [12] J. Antoniadis et al. (EPTA) (2023), 2306.16214.
- [13] Z. Arzoumanian et al. (NANOGrav), *Astrophys. J. Lett.* **905**, L34 (2020), 2009.04496.
- [14] S. Chen et al., *Mon. Not. Roy. Astron. Soc.* **508**, 4970 (2021), 2110.13184.
- [15] B. Goncharov et al., *Astrophys. J. Lett.* **917**, L19 (2021), 2107.12112.
- [16] J. Antoniadis et al., *Mon. Not. Roy. Astron. Soc.* **510**, 4873 (2022), 2201.03980.
- [17] G. Franciolini, A. Iovino, Junior., V. Vaskonen, and H. Veermäe (2023), 2306.17149.
- [18] G. Franciolini, D. Racco, and F. Rompineve (2023), 2306.17136.
- [19] L. Liu, Z.-C. Chen, and Q.-G. Huang (2023), 2307.01102.
- [20] J. Ellis, M. Fairbairn, G. Hütsi, J. Raidal, J. Urrutia, V. Vaskonen, and H. Veermäe (2023), 2306.17021.
- [21] Y.-M. Wu, Z.-C. Chen, and Q.-G. Huang (2023), 2307.03141.
- [22] Y.-Y. Li, C. Zhang, Z. Wang, M.-Y. Cui, Y.-L. S. Tsai, Q. Yuan, and Y.-Z. Fan (2023), 2306.17124.
- [23] S. Sun, X.-Y. Yang, and Y.-L. Zhang, *Phys. Rev. D* **106**, 066006 (2022), 2112.15593.
- [24] A. Afzal et al. (NANOGrav), *Astrophys. J. Lett.* **951**, L11 (2023), 2306.16219.
- [25] H. Middleton, A. Sesana, S. Chen, A. Vecchio, W. Del Pozzo, and P. A. Rosado, *Mon. Not. Roy. Astron. Soc.* **502**, L99 (2021), 2011.01246.
- [26] G. Agazie et al. (NANOGrav), *Astrophys. J. Lett.* **952**, L37 (2023), 2306.16220.
- [27] P. F. Depta, K. Schmidt-Hoberg, P. Schwaller, and C. Tasillo (2023), 2306.17836.
- [28] Y. Gouttenoire, S. Trifinopoulos, G. Valogiannis, and M. Vanvlasselaer (2023), 2307.01457.
- [29] L. Bian, R.-G. Cai, J. Liu, X.-Y. Yang, and R. Zhou, *Phys. Rev. D* **103**, L081301 (2021), 2009.13893.
- [30] Z. Arzoumanian et al. (NANOGrav), *Phys. Rev. Lett.* **127**, 251302 (2021), 2104.13930.
- [31] X. Xue et al., *Phys. Rev. Lett.* **127**, 251303 (2021), 2110.03096.
- [32] D. Wang (2022), 2201.09295.
- [33] D. Wang (2022), 2203.10959.
- [34] R. Z. Ferreira, A. Notari, O. Pujolas, and F. Rompineve, *JCAP* **02**, 001 (2023), 2204.04228.
- [35] K. Inomata, M. Kawasaki, K. Mukaida, and T. T. Yanagida (2023), 2309.11398.
- [36] P. Hunt and S. Sarkar, *JCAP* **12**, 052 (2015), 1510.03338.
- [37] N. Planck Collaboration, Aghanim et al. (Planck), *Astron. Astrophys.* **641**, A6 (2020), [Erratum: *Astron. Astrophys.* 652, C4 (2021)], 1807.06209.
- [38] M. Punturo et al., *Class. Quant. Grav.* **27**, 194002 (2010).
- [39] S. Kawamura et al., *PTEP* **2021**, 05A105 (2021), 2006.13545.
- [40] K. Yagi and N. Seto, *Phys. Rev. D* **83**, 044011 (2011), [Erratum: *Phys. Rev. D* 95, 109901 (2017)], 1101.3940.
- [41] N. Aggarwal et al., *Living Rev. Rel.* **24**, 4 (2021), 2011.12414.
- [42] V. Domcke, C. Garcia-Cely, and N. L. Rodd, *Phys. Rev. Lett.* **129**, 041101 (2022), 2202.00695.
- [43] C.-T. Gao, Y. Gao, Y. Liu, and S. Sun (2023), 2305.00877.
- [44] S. Sun and Y.-L. Zhang, *Phys. Rev. D* **104**, 103009 (2021), 2003.10527.
- [45] K. Inomata and T. Nakama, *Phys. Rev. D* **99**, 043511 (2019), 1812.00674.
- [46] S. Pi and M. Sasaki, *JCAP* **09**, 037 (2020), 2005.12306.
- [47] P. Chen, S. Koh, and G. Tumurtushaa, arXiv e-prints arXiv:2107.08638 (2021), 2107.08638.
- [48] M. Raidal, C. Spethmann, V. Vaskonen, and H. Veermäe, *JCAP* **02**, 018 (2019), 1812.01930.
- [49] G. Hütsi, M. Raidal, V. Vaskonen, and H. Veermäe, *JCAP* **03**, 068 (2021), 2012.02786.
- [50] A. Hall, A. D. Gow, and C. T. Byrnes, *Phys. Rev. D* **102**, 123524 (2020), 2008.13704.
- [51] X.-J. Zhu, E. Howell, T. Regimbau, D. Blair, and Z.-H. Zhu, *Astrophys. J.* **739**, 86 (2011), 1104.3565.
- [52] P. F. de Salas and S. Pastor, *JCAP* **07**, 051 (2016), 1606.06986.
- [53] B. Carr and F. Kuhnel, *Ann. Rev. Nucl. Part. Sci.* **70**, 355 (2020), 2006.02838.
- [54] F. Feroz, M. P. Hobson, and M. Bridges, *Mon. Not. Roy. Astron. Soc.* **398**, 1601 (2009), 0809.3437.
- [55] A. Lewis (2019), 1910.13970.
- [56] P. Amaro-Seoane et al., arXiv e-prints arXiv:1702.00786 (2017), 1702.00786.
- [57] S. Kawamura et al., *Class. Quant. Grav.* **28**, 094011 (2011).
- [58] J. Crowder and N. J. Cornish, *Phys. Rev. D* **72**, 083005 (2005), gr-qc/0506015.
- [59] D. Reitze et al., *Bull. Am. Astron. Soc.* **51**, 035 (2019), 1907.04833.
- [60] J. Aasi et al. (LIGO Scientific), *Class. Quant. Grav.* **32**, 074001 (2015), 1411.4547.
- [61] F. Acernese et al. (VIRGO), *Class. Quant. Grav.* **32**, 024001 (2015), 1408.3978.
- [62] T. Akutsu et al. (KAGRA), *Nature Astron.* **3**, 35 (2019), 1811.08079.
- [63] E. Thrane and J. D. Romano, *Phys. Rev. D* **88**, 124032 (2013), 1310.5300.
- [64] J. García-Bellido, S. Jaraba, and S. Kuroyanagi, *Phys. Dark Univ.* **36**, 101009 (2022), 2109.11376.
- [65] A. Arvanitaki and A. A. Geraci, *Phys. Rev. Lett.* **110**, 071105 (2013), 1207.5320.
- [66] M. Goryachev and M. E. Tobar, *Phys. Rev. D* **90**, 102005 (2014), 1410.2334.
- [67] M. Silva-Feaver et al., *IEEE Trans. Appl. Supercond.* **27**, 1400204 (2017), 1610.09344.
- [68] J. D. Bowman, A. E. E. Rogers, R. A. Monsalve, T. J. Mozdzen, and N. Mahesh, *Nature* **555**, 67 (2018), 1810.05912.
- [69] C. Bartram et al. (ADMX), *Phys. Rev. Lett.* **127**, 261803 (2021), 2110.06096.
- [70] N. Herman, A. Füzfa, L. Lehoucq, and S. Clesse, *Phys. Rev. D* **104**, 023524 (2021), 2012.12189.
- [71] D. J. Fixsen et al., *Astrophys. J.* **734**, 5 (2011), 0901.0555.
- [72] G. Franciolini, A. Maharana, and F. Muia, *Phys. Rev. D* **106**, 103520 (2022), 2205.02153.
- [73] P. Auclair et al. (LISA Cosmology Working Group), *Living Rev. Rel.* **26**, 5 (2023), 2204.05434.
- [74] V. Vaskonen and H. Veermäe, *Phys. Rev. D* **101**, 043015

- (2020), 1908.09752.
- [75] K. Ando, K. Inomata, and M. Kawasaki, Phys. Rev. D **97**, 103528 (2018), 1802.06393.
- [76] K. Kohri and T. Terada, Phys. Rev. D **97**, 123532 (2018), 1804.08577.
- [77] E. W. Kolb and M. S. Turner, *The early universe*, vol. 69 (CRC press, 1990).
- [78] B. Wallisch, Ph.D. thesis, Cambridge U. (2018), 1810.02800.
- [79] B. J. Carr, K. Kohri, Y. Sendouda, and J. Yokoyama, Phys. Rev. D **81**, 104019 (2010), 0912.5297.
- [80] T. Nakama, J. Silk, and M. Kamionkowski, Phys. Rev. D **95**, 043511 (2017), 1612.06264.
- [81] O. Özsoy, S. Parameswaran, G. Tasinato, and I. Zavala, JCAP **07**, 005 (2018), 1803.07626.
- [82] S. Young, C. T. Byrnes, and M. Sasaki, JCAP **07**, 045 (2014), 1405.7023.
- [83] B. J. Carr, Astrophys. J. **201**, 1 (1975).
- [84] I. Musco and J. C. Miller, Class. Quant. Grav. **30**, 145009 (2013), 1201.2379.
- [85] T. Harada, C.-M. Yoo, and K. Kohri, Phys. Rev. D **88**, 084051 (2013), 1309.4201.